Data in Brief 39 (2021) 107484

Contents lists available at ScienceDirect

Data in Brief

journal homepage: www.elsevier.com/locate/dib

Data Article

Imaging data reveal divergent longitudinal trajectories in PLS, ALS and poliomyelitis survivors: Group-level and single-subject traits

Marlene Tahedl[a,b], Stacey Li Hi Shing[a], Eoin Finegan[a], Rangariroyashe H. Chipika[a], Jasmin Lope[a], Aizuri Murad[a], Orla Hardiman[a], Peter Bede[a,c,*]

[a] Computational Neuroimaging Group, Trinity Biomedical Sciences Institute, Trinity College Dublin, Pearse Street Room 5.43, Dublin, Ireland
[b] Department of Psychiatry and Psychotherapy and Institute for Psychology, University of Regensburg, Germany
[c] Pitié-Salpêtrière University Hospital, Sorbonne University, Paris, France

ARTICLE INFO

Article history:
Received 24 August 2021
Revised 28 September 2021
Accepted 11 October 2021
Available online 14 October 2021

Keywords:
Motor neuron disease
Amyotrophic lateral sclerosis
Primary lateral sclerosis
Poliomyelitis
Neuroimaging
Clinical trials

ABSTRACT

Imaging profiles from a longitudinal single-centre motor neuron disease study are presented. A standardized T1-weighted MRI protocol was implemented to characterise cortical disease burden trajectories across the UMN (upper motor neuron) - LMN (lower motor neuron) spectrum of motor neuron diseases (MNDs) (Tahedl et al., 2021). Patients with amyotrophic lateral sclerosis (ALS $n = 61$), patients with primary lateral sclerosis (PLS $n = 23$) and poliomyelitis survivors (PMS $n = 45$) were included. Up to four longitudinal scans were available for each patient, separated by an inter-scan-interval of four months. Individual and group-level cortical thickness profiles were appraised using a normalisation procedure with reference to subject-specific control groups. A *z*-scoring approach was utilised, where each patients' cortex was first segmented into 1000 cortical regions, and then rated as 'thin', 'thick', or 'comparable' to the corresponding region of a demographically-matched control cohort. Fractions of significantly 'thin' and 'thick' patches were calculated

DOI of original article: 10.1016/j.neurobiolaging.2021.04.031
* Corresponding author at: Computational Neuroimaging Group, Trinity Biomedical Sciences Institute, Trinity College Dublin, Pearse Street Room 5.43, Dublin, Ireland.
E-mail address: bedep@tcd.ie (P. Bede).

https://doi.org/10.1016/j.dib.2021.107484

across the entire cerebral vertex as well as in specific brain regions, such as the motor cortex, parietal, frontal and temporal cortices. This approach allows the characterisation of disease burden in individual subjects as well as at a group-level, both cross-sectionally and longitudinally. The presented framework may aid the interpretation of individual cortical disease burden in other patient cohorts.

Specifications Table

Subject	Clinical neurology
Specific subject area	Magnetic resonance imaging, Quantitative neuroimaging, Cortical thickness, Motor neuron disease, Amyotrophic Lateral Sclerosis
Type of data	High-resolution T1-weighted magnetic resonance imaging (MRI) data acquired using a standardized acquisition protocol was used to calculate measures of cortical disease burden.
How data were acquired	Magnetic resonance imaging: quantitative neuroimaging metrics retrieved form a standardised acquisition protocol on a 3 Tesla Philips Achieva system using an 8-channel head coil (Philips Medical Systems, Best, The Netherlands)
Data format	Cortical thickness measures are provided as raw values (in millimetres); thin/thick patch counts are given as fractions (indicating, per subject, how many of all patches spanning the distinct cortices were affected)
Parameters for data collection	Local acquisition protocol for patients and healthy controls: 3D T1-weighted sequence: spatial resolution: 1 × 1 × 1 mm, Field of view: 256 × 256 × 160 mm, repetition time (TR) = 8.5 ms, echo time (TE) = 3.9 ms, Inversion time (TI) = 1060 ms, flip angle (FA) = 8°, SENSE factor = 1.5 Cam-CAN database parameters: spatial resolution 1 × 1 × 1 mm, FOV = 256 × 240 × 192 mm, TR/TE 2.25/2.99 ms, TI 900 ms, FA 9°, GRAPPA factor 2.
Description of data collection	Data were collected on a 3 Tesla MRI system. Demographic variables were recorded before the MRI scan, and a standardised neurological examination was also performed on the day of the MRI.
Data source location	Institution: Computational neuroimaging group, Trinity Biomedical Sciences Institute, Trinity College Dublin City/Town/Region: Dublin Country: Ireland
Data accessibility	Raw cortical thickness and thin/thick patch fractions per subject and session data are available online at Mendeley Data; https://data.mendeley.com/datasets/3pnp4hkhnw/1
Related research article	Tahedl M, Li Hi Shing S, Finegan E, Chipika RH, Lope J, Hardiman O, Bede P. Propagation patterns in motor neuron diseases: individual and phenotype-associated disease-burden trajectories across the UMN-LMN spectrum of MNDs. Neurobiol Aging. 2021 In Press

Value of the Data

- Cortical thickness values permit the interpretation of individual cortical thinning profiles in other neurological conditions.
- Regional 'thin-patch' fractions allow the characterisation of atrophy patterns in other conditions across the spectrum of motor neuron diseases.
- The presented statistical framework and methodological description may aid individualised data interpretation in other neurodegenerative conditions.
- Data may be incorporated in meta-analyses to probe the generalizability of our findings.
- Control data offer reference values for the interpretation of 'external' patient data.

1. Data Description

Anatomical patterns of cortical disease burden were evaluated in three patient cohorts across the spectrum of motor neuron diseases (MNDs): 61 patients with amyotrophic lateral sclerosis ('ALS': 43 males, age: 60.20+/– 9.62), 23 patients with primary lateral sclerosis ('PLS': 12 males, age: 58.52 ± 9.79), and 45 poliomyelitis-survivors ('PMS': 20 males, age: 66.07 ± 6.52). To characterise anatomical progression patterns, longitudinal data were also analysed. Cortical thickness values for up to four scans are presented per patient using a uniform inter-scan interval of four months. In Fig. 1, the availability of baseline and follow-up scans is presented in each clinical cohort (Fig. 1). Cross-sectional patient data were first contrasted to pooled normative

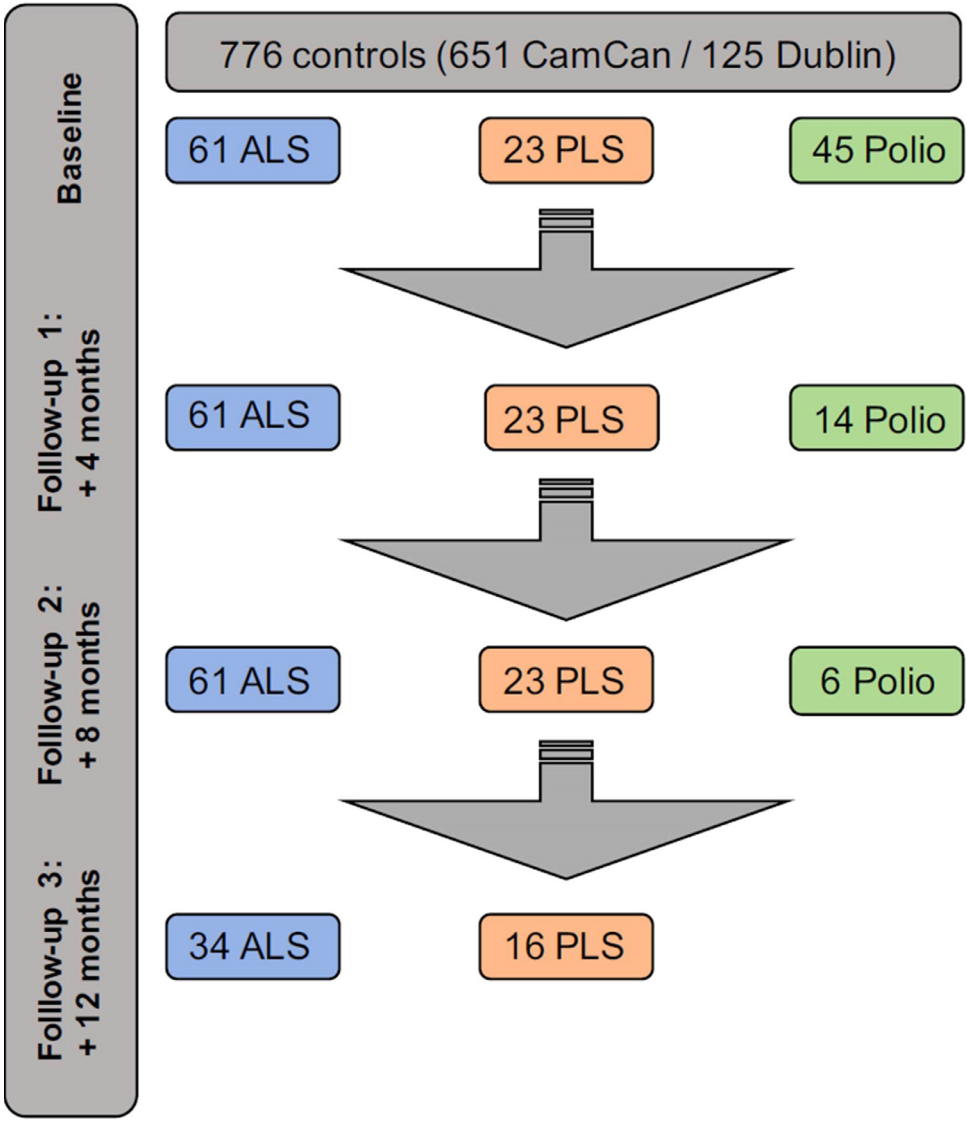

Fig. 1. Flow diagram indicating the number of patients in each study group at each timepoint.

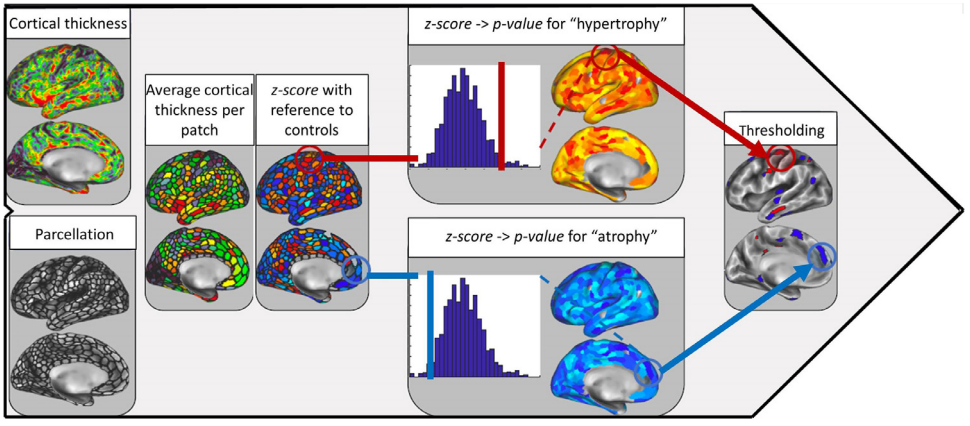

Fig. 2. Flow chart illustrating the methodological framework for calculating 'thin' and 'thick' patch load. Please see text for specific details (section experimental design, materials and methods).

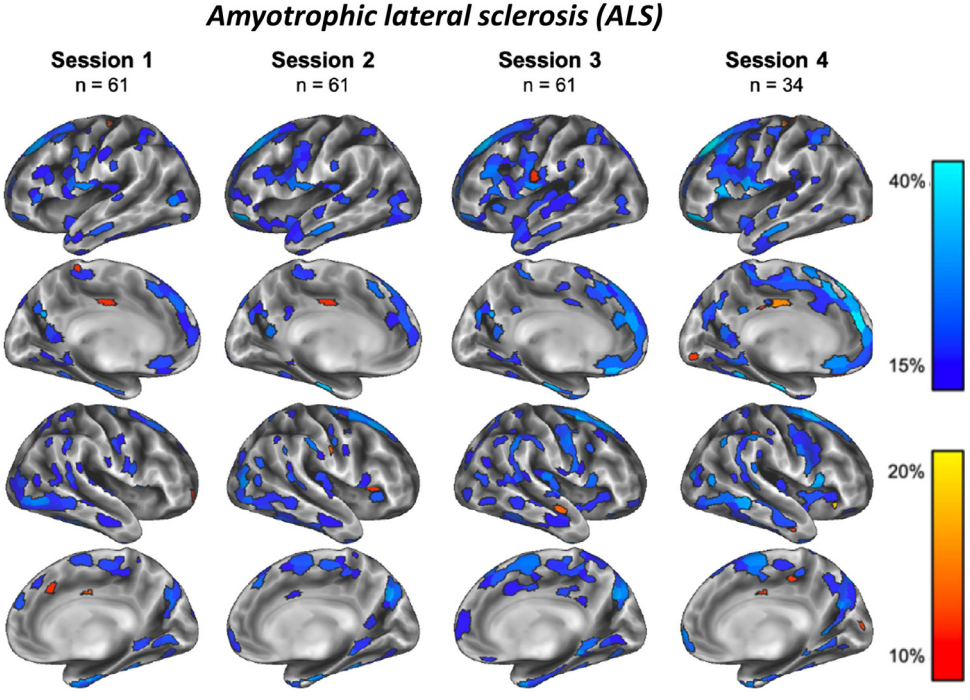

Fig. 3. The statistical brain maps of patients with amyotrophic lateral sclerosis (ALS) depicting the percentage of subjects exhibiting cortical thinning/hypertrophy in each cortical region, at each timepoint. Cool colours indicate cortical atrophy, hot colours refer to thick patches with respect to controls.

data set of healthy controls ('HC', $n = 776$, 383 males, age: 55.08 ± 17.63) from Trinity College Dublin ($n = 125$) and subjects from the Cambridge Centre for Ageing and Neuroscience (Cam-CAN) database ($n = 651$) [2]. The cortical thickness profile of the healthy controls scanned at our institution is presented in the accompanying data sets. As described in the companion article [1], the fraction of significantly 'thin' and 'thick' patches was calculated in each patient by comparing

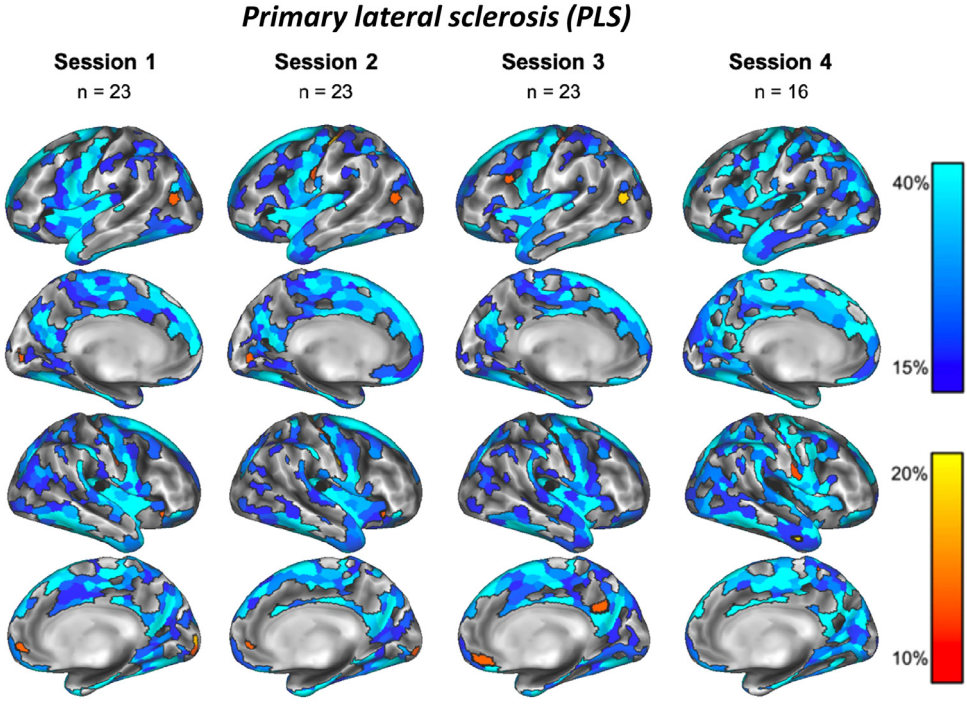

Fig. 4. The statistical brain maps of patients with primary lateral sclerosis (PLS) depicting the percentage of subjects exhibiting cortical thinning/hypertrophy in each cortical region, at each timepoint. Cool colours indicate cortical atrophy, hot colours refer to thick patches with respect to controls.

individual cortical thickness maps to an age- and sex-matched control group. The flowchart for retrieving these metrics is presented in Fig. 2 which provides a step-by-step illustration of the methodological framework (Fig. 2). Our approach not only enabled the characterisation of disease burden in individual patients, but provided descriptive statistics for each patient group at each timepoint. As illustrated in Figs. 3–5**,** the colour coding indicates the percentage of patients in each group at each timepoint exhibiting statistically 'thin' or 'thick' patches in specific cortical regions (Figs. 3–5). Finally, the regional distribution of 'thin' and 'thick' patch load was also evaluated in each cortical region; in the motor, parietal, frontal, and temporal cortices. Cortical thin-patch burden in specific cerebral regions is presented as the radar charts (Fig. 6) across the three diagnostic groups (Fig. 6). The raw data which was utilised to calculate this distribution is available online at https://data.mendeley.com/datasets/3pnp4hkhnw/1. In the companion article, we also present 'standard' cortical thickness analyses, where the cortical thickness profile of the patient groups are contrasted to healthy controls, correcting for age and gender [1].

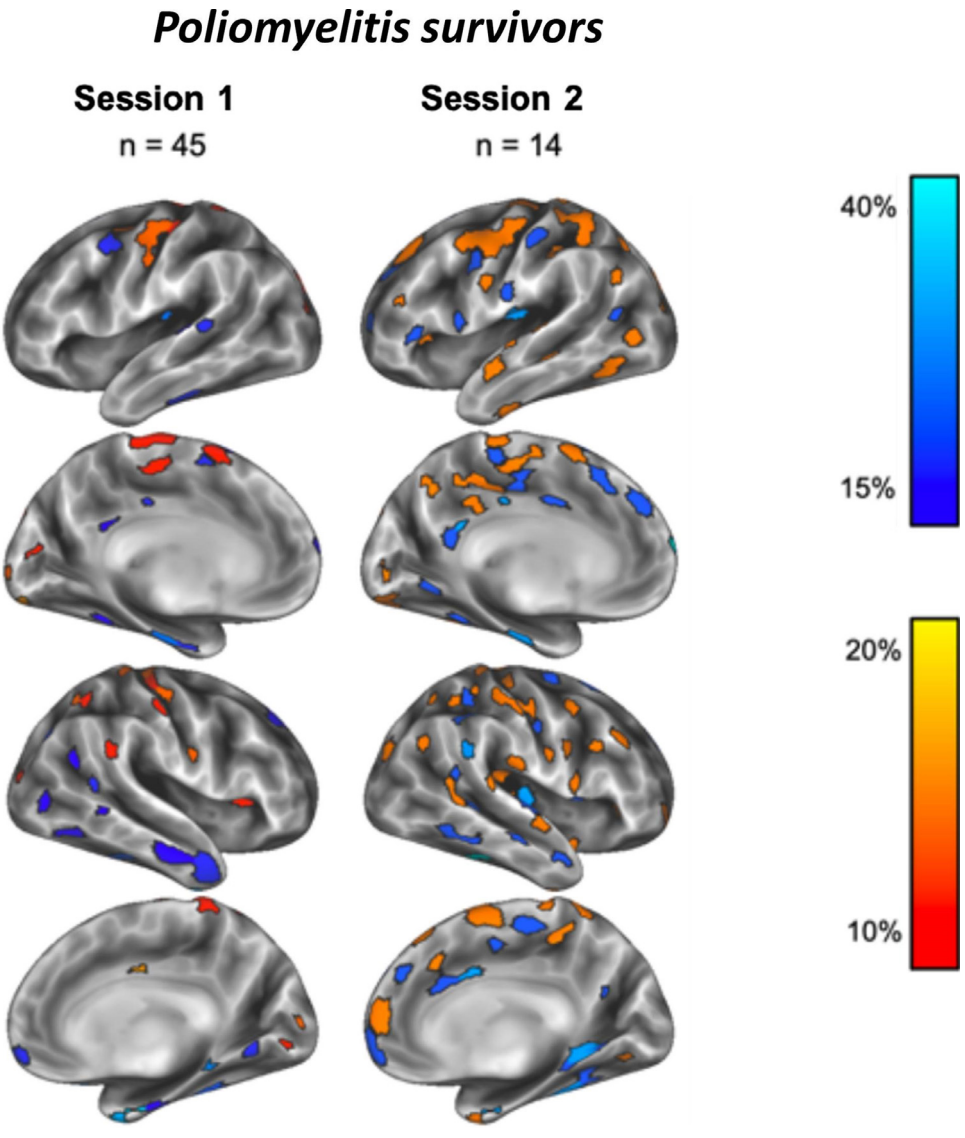

Fig. 5. The statistical brain maps of poliomyelitis survivors depicting the percentage of subjects exhibiting cortical thinning/hypertrophy in each cortical region, at each timepoint. Cool colours indicate cortical atrophy, hot colours refer to thick patches with respect to controls.

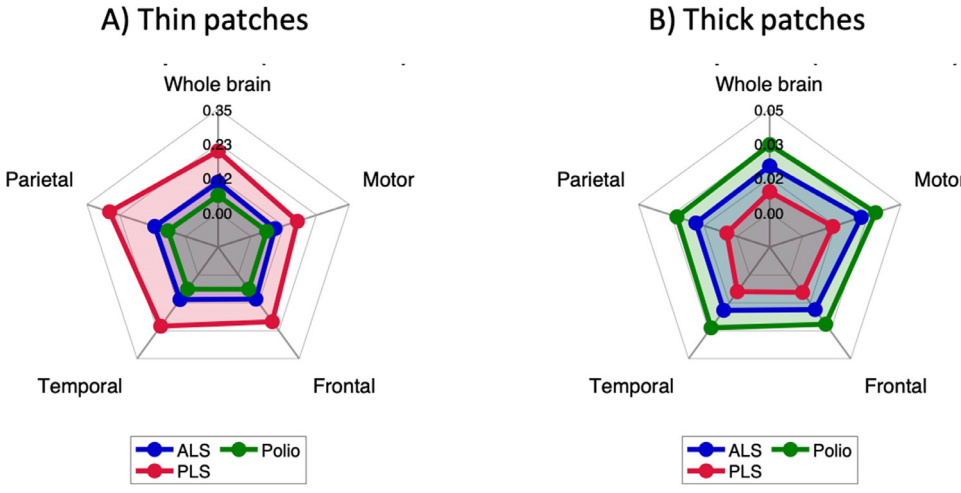

Fig. 6. Radar charts illustrating the topographical distribution of cortical disease burden in the different patient groups at baseline comparisons. Thin (A) and thick (B) patch fractions are presented for the entire brain and the motor, parietal, frontal and temporal cortices.

2. Experimental Design, Materials and Methods

Motor neuron diseases encompass a range of clinically heterogeneous conditions, with considerable differences in clinical [3,4], radiological [5–7] and biomarker profiles [8–10]. While the radiological features of amyotrophic lateral sclerosis are well established [11,12], distinguishing imaging patterns in upper motor neuron predominant MNDs [13–15] and lower motor neuron predominant MNDs [16–18] are less well characterised. Machine-learning applications are increasingly utilised to interpret single MRI scans in motor neuron diseases [19], but the radiological distinction between ALS and PLS remains challenging [20–22] without the evaluation of spinal cord metrics [23,24]. Accordingly, in this study T1-weighted MRI data from 129 patients were included spanning the UMN-LMN spectrum of motor neuron diseases: 61 patients with amyotrophic lateral sclerosis (ALS), 23 patients with primary lateral sclerosis (PLS) and 45 poliomyelitis survivors (PMS). Data from multiple timepoints were available for each patient, acquired 4 months apart (Fig. 1). The research has been carried out in accordance with The Code of Ethics of the World Medical Association (Declaration of Helsinki) and all patients provided informed consent in accordance with the ethics approval of the study (Medical Research Committee of Beaumont Hospital, Dublin, Ireland). ALS patients had 'probable' or 'definite' ALS according to the El Escorial criteria [25] and PLS patients were diagnosed based on the Gordon criteria [26]. A large, pooled control dataset ($n = 776$) was utilised to interpret patient data. The total number and fraction of significantly 'thin' and 'thick' patches were calculated as follows (Fig. 2): First, surface-based cortical thickness maps were obtained using FreeSurfer's *recon-all* pipeline on individual T1-weigthed MRI data, which were then converted into the Connectivity Informatics Technology Initiative (CIFTI) file format using the *CIFTIFY* toolbox [27] for visualization. Subsequently, the cortex was segmented into 1000 equally-sized region, and cortical thickness was averaged in a cortical 'patch'. These maps were then converted into z-maps, with respect to an age- and sex- matched control group, encompassing sex-matched healthy controls with an age range of +/− 2 years of the individual patient. Finally, p-values were obtained from the z-scores using a Monte-Carlo permutation procedure, which is describe in more details in the companion article [1]. As both p-values representing the probability of higher and lower cortical thickness were calculated (representing focal atrophy or hypertrophy) p-maps were thresholded at $a = 0.05/2 = 0.025$. The number of whole-brain 'thin'/'thick' patches was then converted

to fractions by dividing by the total number of patches. To characterise the regional profile of phenotype-associated atrophy, this procedure was repeated restricted to 'patches' within the (1) motor, (2) parietal, (3) frontal and (4) temporal cortices using the Desikan-Kiliany atlas [28] to define these anatomical regions.

Ethics Statement

This study was approved by the Medical Research Committee of Beaumont Hospital, Dublin, Ireland. All participants provided informed consent prior to participation.

Declaration of Competing Interest

The authors have no competing financial interests or personal relationships to declare which may be construed as conflict of interest.

CRediT Author Statement

Marlene Tahedl: Conceptualization, Methodology, Formal analysis, Writing – original draft; **Stacey Li Hi Shing:** Investigation, Writing – review & editing; **Eoin Finegan:** Investigation, Writing – review & editing; **Rangariroyashe H. Chipika:** Investigation, Writing – review & editing; **Jasmin Lope:** Formal analysis, Investigation, Writing – review & editing; **Aizuri Murad:** Formal analysis, Investigation, Writing – review & editing; **Orla Hardiman:** Investigation, Writing – review & editing; **Peter Bede:** Conceptualization, Methodology, Formal analysis, Writing – original draft.

Acknowledgments

We are grateful for the participation of each patient and healthy control, and we also thank all the patients who expressed interest in this research study but were unable to participate for medical or logistical reasons.

Funding Statement

This study was sponsored by the Spastic Paraplegia Foundation (SPF). Professor Peter Bede and the Computational Neuroimaging Group are also supported by the Health Research Board (HRB EIA-2017-019), the Irish Institute of Clinical Neuroscience (IICN), the EU Joint Programme – Neurodegenerative Disease Research (JPND), the Andrew Lydon scholarship, and the Iris O'Brien Foundation.

References

[1] M. Tahedl, et al., Propagation patterns in motor neuron diseases: individual and phenotype-associated disease-burden trajectories across the UMN-LMN spectrum of MNDs, Neurobiol. Aging (2021) In Press, doi:10.1016/j.neurobiolaging.2021.04.031.
[2] M.A. Shafto, et al., The Cambridge Centre for ageing and neuroscience (Cam-CAN) study protocol: a cross-sectional, lifespan, multidisciplinary examination of healthy cognitive ageing, BMC Neurol. 14 (2014) 204.
[3] E. Finegan, et al., Pathological crying and laughing in motor neuron disease: pathobiology, screening, intervention, Front. Neurol. 10 (2019) 260.
[4] T. Burke, et al., Discordant performance on the 'Reading the Mind in the Eyes' Test, based on disease onset in amyotrophic lateral sclerosis, Amyotroph. Lateral Scler. Frontotemporal Degener. 17 (2016) 467–472, doi:10.1080/21678421.2016.1177088.

[5] F. Christidi, et al., Clinical and radiological markers of extra-motor deficits in amyotrophic lateral sclerosis, Front. Neurol. 9 (2018) 1005.
[6] E. Verstraete, et al., Mind the gap: the mismatch between clinical and imaging metrics in ALS, Amyotroph. Lateral Scler. Frontotemporal Degener. 16 (7-8) (2015) 524–529.
[7] T. Burke, et al., Measurement of social cognition in amyotrophic lateral sclerosis: a population based study, PLoS ONE 11 (8) (2016) e0160850.
[8] H. Blasco, et al., A pharmaco-metabolomics approach in a clinical trial of ALS: identification of predictive markers of progression, PLoS ONE 13 (6) (2018) e0198116.
[9] M. Feron, et al., Extrapyramidal deficits in ALS: a combined biomechanical and neuroimaging study, J. Neurol. 265 (9) (2018) 2125–2136.
[10] S. Dukic, et al., Patterned functional network disruption in amyotrophic lateral sclerosis, Hum. Brain Mapp. 40 (16) (2019) 4827–4842.
[11] F. Christidi, et al., Hippocampal pathology in amyotrophic lateral sclerosis: selective vulnerability of subfields and their associated projections, Neurobiol. Aging 84 (2019) 178–188.
[12] B. Nasseroleslami, et al., Characteristic increases in EEG connectivity correlate with changes of structural MRI in amyotrophic lateral sclerosis, Cereb. Cortex 29 (1) (2019) 27–41.
[13] E. Finegan, et al., The clinical and radiological profile of primary lateral sclerosis: a population-based study, J. Neurol. 266 (11) (2019) 2718–2733.
[14] P. Bede, et al., Brainstem pathology in amyotrophic lateral sclerosis and primary lateral sclerosis: a longitudinal neuroimaging study, Neuroimage Clin. 24 (2019) 102054.
[15] M. Abidi, et al., Adaptive functional reorganization in amyotrophic lateral sclerosis: coexisting degenerative and compensatory changes, Eur. J. Neurol. 27 (1) (2020) 121–128.
[16] M.V. Lebouteux, et al., Revisiting the spectrum of lower motor neuron diseases with snake eyes appearance on magnetic resonance imaging, Eur. J. Neurol. 21 (9) (2014) 1233–1241.
[17] G. Querin, et al., The spinal and cerebral profile of adult spinal-muscular atrophy: a multimodal imaging study, Neuroimage Clin. 21 (2019) 101618.
[18] S. Li Hi Shing, et al., Post-polio syndrome: more than just a lower motor neuron disease, Front. Neurol. 10 (2019) 773.
[19] G. Querin, et al., Multimodal spinal cord MRI offers accurate diagnostic classification in ALS, J. Neurol. Neurosurg. Psychiatry 89 (11) (2018) 1220–1221.
[20] E. Finegan, et al., Widespread subcortical grey matter degeneration in primary lateral sclerosis: a multimodal imaging study with genetic profiling, Neuroimage Clin. 24 (2019) 102089.
[21] P. Bede, G. Querin, P.F. Pradat, The changing landscape of motor neuron disease imaging: the transition from descriptive studies to precision clinical tools, Curr. Opin. Neurol. 31 (4) (2018) 431–438.
[22] R.H. Chipika, et al., Switchboard malfunction in motor neuron diseases: selective pathology of thalamic nuclei in amyotrophic lateral sclerosis and primary lateral sclerosis, Neuroimage Clin. 27 (2020) 102300.
[23] M.M. El Mendili, et al., Spinal cord imaging in amyotrophic lateral sclerosis: historical concepts-novel techniques, Front. Neurol. 10 (2019) 350.
[24] G. Querin, et al., Presymptomatic spinal cord pathology in c9orf72 mutation carriers: a longitudinal neuroimaging study, Ann. Neurol. 86 (2) (2019) 158–167.
[25] B.R. Brooks, et al., El Escorial revisited: revised criteria for the diagnosis of amyotrophic lateral sclerosis, Amyotroph. Lateral Scler. Motor Neuron Disord. 1 (5) (2000) 293–299.
[26] P.H. Gordon, et al., The natural history of primary lateral sclerosis, Neurology 66 (5) (2006) 647–653.
[27] E.W. Dickie, et al., Ciftify: a framework for surface-based analysis of legacy MR acquisitions, Neuroimage 197 (2019) 818–826.
[28] R.S. Desikan, et al., An automated labeling system for subdividing the human cerebral cortex on MRI scans into gyral based regions of interest, Neuroimage 31 (3) (2006) 968–980.